Quality Assurance and Stability Reference (QUASAR) Monitoring Results for Six Earth Observation Sensors Using Airborne Hyperspectral Data

P.M. Teillet [1], G. Fedosejevs [1], R.P. Gauthier [1], R.T. Shin [1],
N.T. O'Neill [2], K.J. Thome [3], and A. Meygret [4]

1. Canada Centre for Remote Sensing, 588 Booth Street,
Ottawa, Ontario, Canada K1A 0Y7

2. CARTEL, Université de Sherbrooke,
Sherbrooke, Québec, Canada J1K 2R1

3. Optical Sciences Center, University of Arizona,
Tucson, Arizona, USA 85721-0094

4. Centre national d'études spatiales, BPI 811, 18, avenue Edouard Bélin,
31401 Toulouse, Cedex 4, France

ABSTRACT

This paper reports on experimental work to test the feasibility of using reference hyperspectral data sets to carry out vicarious radiometric calibrations for multiple satellite sensors. The methodology has been validated using data from a campaign at the Railroad Valley playa test site in Nevada. The proof of concept has been further tested based on two data acquisition campaigns at the Newell County rangeland test site in Alberta. All three campaigns included ground-based measurements, satellite imagery, and airborne hyperspectral data. The airborne image data were acquired using the AVIRIS sensor in Nevada and the *casi* sensor in all three cases. Radiometric calibration monitoring results were obtained for six sensors: NOAA-14 AVHRR, Landsat-5 TM, SPOT-1 HRV, SPOT-2 HRV, SPOT-4 VGT, and OrbView-2 SeaWiFS. These results indicate that the nominal on-orbit radiometric calibrations of all the satellite sensors fit within their predicted uncertainties. The combination of both lower-reflectance and higher-reflectance test sites is shown to improve the quality of the calibration monitoring results.

Keywords: Sensor radiometric calibration; vicarious calibration; test sites; hyperspectral remote sensing.

I. INTRODUCTION

Experimental work is being done to test the feasibility of using single hyperspectral data sets to carry out vicarious calibrations for multiple sensors. The domain of interest and applicability is that of optical sensors with spectral bands in the range encompassed by the reference hyperspectral sensor. The approach is applicable to sensors with large footprints (1-km, for example) and small footprints (20-m, for example). Such a capability has the potential to provide timely monitoring of quality assurance and stability reference (QUASAR) test sites for calibration purposes

QUASAR monitoring data acquisition campaigns took place at the Railroad Valley playa test site in Nevada on June 17, 1998, and at the Newell County rangeland test site in Alberta on August 4, 1998 and October 4, 1998. Ground-based measurements, satellite imagery, and airborne hyperspectral data were acquired in all cases. The airborne imagery was obtained using the Compact Airborne Spectrographic Imager (*casi*™) for all three campaigns and the Airborne Visible Infrared Imaging Spectrometer (AVIRIS) in addition for the Railroad Valley campaign. The ground-based measurements included spectral data obtained using the GER3700™ spectrometer for all three campaigns and the ASD FieldSpec™ spectrometer in addition for the Railroad Valley campaign.

The airborne hyperspectral data sets were used to generate radiometric calibration estimates for selected spectral bands of six Earth observation sensors that imaged the test sites on or near the three airborne data acquisition dates. The principal results consist of comparisons of top-of-atmosphere radiances predicted by QUASAR to nominal values obtained from the actual satellite sensor image data. The satellite sensors and the relevant spectral bands are NOAA-14 AVHRR (spectral band 1), Landsat-5

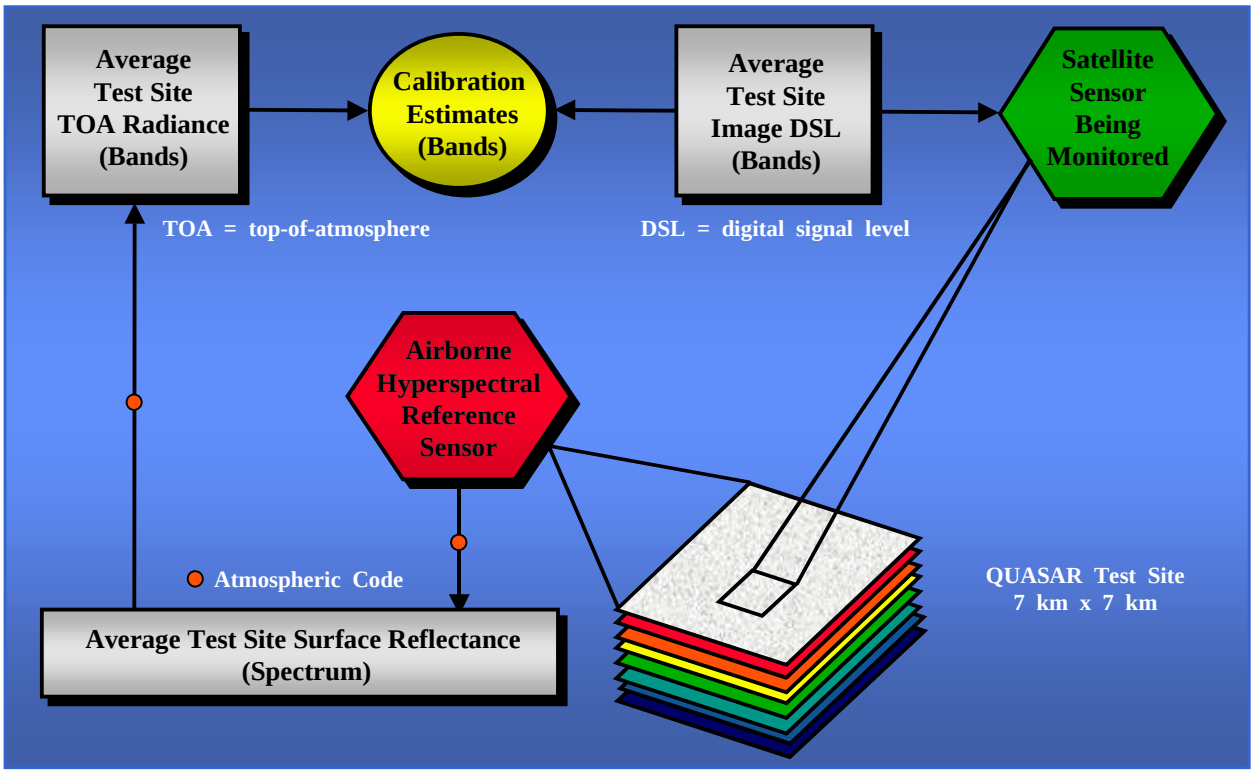

Figure 1. The QUASAR concept for monitoring satellite sensor calibration. An airborne reference sensor is used for methodology prototyping and interim operations while waiting for well-calibrated hyperspectral satellite sensors to become available.

TM (spectral bands 1-4), SPOT-1 and SPOT-2 HRV (spectral bands 1-3), SPOT-4 VGT (spectral bands 1-3 (i.e., B0, B2, and B3)), and SeaWiFS (spectral bands 1-8).

II. THE QUASAR APPROACH

The QUASAR methodology (Teillet et al. 2000) is briefly summarized as follows. Airborne mission and field measurement methodologies have been created to acquire spatially extensive hyperspectral imagery over selected test sites (Figure 1) as well as ground-level ancillary and validation data sets. As Figure 1 also portrays, it will be possible to attempt QUASAR monitoring using well-calibrated satellite hyperspectral sensors when they become available. A data processing and analysis scheme has been formulated and implemented in prototype mode to retrieve an average surface reflectance spectrum for the test site under consideration and to predict top-of-atmosphere (TOA) radiances for satellite sensors of interest for calibration monitoring purposes.

The Imaging Spectrometer Data Analysis System (ISDAS) (Staenz et al. 1998) at the Canada Centre for Remote Sensing was used to carry out the atmospheric computations using the Modtran-3 radiative transfer code and a look-up table approach (Staenz and Williams 1997). Atmospheric correction errors are expected to be negligible for the transfer between the reference and the monitored sensors because of the two-way radiative transfer computations (see Section IV).

The hyperspectral and spatially extensive nature of QUASAR benchmark data sets makes it possible to attempt vicarious calibrations for any sensor(s) with appropriate characteristics that imaged the test site on the same day, or within a day or two if atmospheric and surface conditions have not changed significantly. Appropriate sensors include any with footprints that fit comfortably within the test site and with one or more spectral bands encompassed by the wavelength coverage of the airborne hyperspectral sensor. Spectral bands outside the wavelength range of the reference sensor can be monitored using inter-band relative calibration methods.

A detailed error budget analysis is in progress to assess the accuracy of the QUASAR approach (Bergeron et al. 1998). Scott et al. (1996) have estimated that the uncertainty in using the Railroad

Valley playa for cross-calibration with respect to a reference sensor is on the order of ± 6.1 percent (one sigma) (Scott et al. 1996). This error estimate is based on the root sum squares of errors from four sources: the reference sensor calibration (4.9 percent (Biggar et al., 1994)), image registration (2.5 percent), spectral correction (2.0 percent), and reflectance anisotropy correction (1.7 percent).

As described in greater detail in the next Section, the nominal sensor set for experimental QUASAR monitoring to date has consisted of an airborne *casi*, a GER3700 ground spectrometer, and a Microtops II sunphotometer. If the method proves to be feasible, the need for ground-based measurements could be reduced to sunphotometer measurements only, preferably using an automated station deployed at a test site, or possibly a multi-altitude approach to the determination of atmospheric aerosol optical parameters.

III. TEST SITES AND DATA SETS

The test sites in the Railroad Valley and Newell County areas are both 7 km by 7 km in size and are described in greater detail by Teillet et al. (1998a, 1998b, 2000). Radiometric uniformity studies were used to determine the location and size of these primary test sites (Teillet et al. 1998b).

The Railroad Valley playa in Nevada (hereafter referred to as RVPN) is situated at 38° 28' N and 115° 41' W and at an elevation of 1435 m above sea level (ASL). The playa is very flat and homogeneous and consists of compacted clay-rich lacustrine deposits forming a relatively smooth surface compared to most land covers. It has a growing history of international use as a test site for vicarious calibration and it serves as a good setting for QUASAR methodology validation.

The prairie rangeland test site is in Newell County, Alberta (hereafter referred to as NCRA), which is north-west of Medicine Hat, Alberta. The test site is located at 50° 18' N and 111° 38' W and has a terrain elevation of 750 m ASL. Given its reasonable proximity to urban areas from which hyperspectral sensors can be flown (a few hundred kilometers) and its lower reflectance compared to desert sites, Newell County rangeland in Alberta has the potential to serve as a routine test site for interim performance monitoring of satellite sensors (Teillet et al. 2000).

Remote Sensing Data Sets at RVPN

For the RVPN QUASAR test site, near-coincident satellite sensor imagery was acquired on the *casi* and AVIRIS flight day, June 17, 1998, by NOAA-14 AVHRR, Orbview-2 SeaWiFS, and SPOT-4 VGT. SPOT-1 HRV data were acquired on the next day, whereas Landsat-5 TM data were acquired three days prior to the airborne data acquisition day. Other NOAA-14 AVHRR data were also acquired within a few days of June 17.
The airborne *casi* imagery was acquired at a flight altitude of 3400 meters above sea level (1965 meters above ground level) such that the spatial resolution of the data is approximately 2.6 meters. Eleven parallel flight lines were used to cover the 7 km by 7 km test site.

The airborne AVIRIS imagery was acquired at a flight altitude of 20.8 kilometres above sea level (19.3 kilometres above ground level) such that the spatial resolution of the data is approximately 17.5 meters. A single flight line was needed to cover the 7 km by 7 km test site.

Remote Sensing Data Sets at NCRA

For the August NCRA data acquisition campaign, near-coincident satellite sensor imagery was acquired on the *casi* flight day, August 4, 1998, by NOAA-14 AVHRR, and OrbView-2 SeaWiFS. SPOT-4 VGT and other AVHRR and SeaWiFS data were also acquired within a few days of August 4. SPOT-2 HRV and Landsat-5 TM data were acquired three and four days, respectively, after the airborne data acquisition day.

For the October NCRA data acquisition campaign, near-coincident satellite sensor imagery was acquired on the *casi* flight day, October 4, 1998, by NOAA-14 AVHRR, OrbView-2 SeaWiFS, SPOT-4 VGT, Landsat-5 TM, and SPOT-2 HRV. Other AVHRR, VGT, and SeaWiFS data were also acquired within a few days of October 4.

For both NCRA campaigns, the airborne *casi* imagery was acquired at a flight altitude of 3000 meters above sea level (2245 meters above ground level) such that the spatial resolution of the data is approximately 3 meters. Eleven parallel flight lines were used to cover the 7 km by 7 km test site.

Ground-Based Data Sets at Both Test Sites

A 100-meter by 100-meter ground validation site within the 7 km by 7 km test was selected at both test sites for ground-based measurements. In all cases, these measurements included GER3700 spectrometer measurements made over the surface and over a Labsphere Spectralon™ reflectance panel to generate surface reflectances for use in validating surface reflectances retrieved from the airborne hyperspectral imagery. At the RVPN test site, the ground-based measurements also included FieldSpec spectrometer measurements made over the surface and over a Spectralon reflectance panel to generate surface reflectances for use as an independent validation of surface reflectances retrieved from the GER spectrometer and the airborne hyperspectral imagery. Both of the aforementioned reflectance panels were calibrated radiometrically and characterized for bi-directional reflectance properties in the laboratory at the University of Arizona.

Sun photometer measurements were made from the centre of the validation site using a hand-held, calibrated Microtops-II ™ sunphotometer during the satellite and aircraft sensor overpasses. The resulting data were used to obtain atmospheric aerosol optical depth at 0.550 micrometers (AOD550). For the RVPN test site on June 17, 1998, this yielded a characteristic value of AOD550 = 0.04. For the NCRA test site, the characteristic value of AOD550 on 4 August 1998 was 0.09. Despite plans to the contrary, sunphotometer measurements were not available during the October data acquisition campaign. Atmospheric conditions were clear and a value of 0.05 was assumed for AOD550. At the RVPN test site, sunphotometer measurements were also made using a well-calibrated, tripod-mounted Reagan solar radiometer. A comparison of Microtops-II and Reagan sunphotometer measurements over the course of several days at the RVPN test site showed differences in retrieved AOD550 averaging 0.01 and not exceeding 0.03.

IV. DATA PROCESSING

The main data processing steps are summarized in Figure 2 (Teillet et al. 2000). It is assumed that the TOA radiance estimates obtained from the QUASAR methodology (i.e., the output of the last step in the data flow diagram) for the various satellite sensor spectral bands are representative of the entire 7-km by 7-km test site. Thus, digital signal levels (DSL, in counts) can be extracted from relevant satellite sensor images of the test sites and combined with the QUASAR TOA radiances to generate estimates of radiometric calibration gain coefficients in counts per unit radiance. With a reference area of 7 km by 7 km, it is possible to accommodate several image pixels even for large footprint sensors and still stay well within the boundaries of the area to allow for location errors. For comparison, the nominal post-launch calibration coefficients were obtained from the pertinent sources. For AVHRR, the coefficients were from the NASA Goddard Space Flight Center and based on ocean and cloud scene methodologies (Vermote and Kaufman 1998). For SeaWiFS, the calibration was obtained by running the SeaWiFS Data Analysis System (SeaDAS) package (Fu et al. 1998). For TM, HRV, and VGT, the nominal calibration coefficients were taken from the product tape header and/or the product documentation.

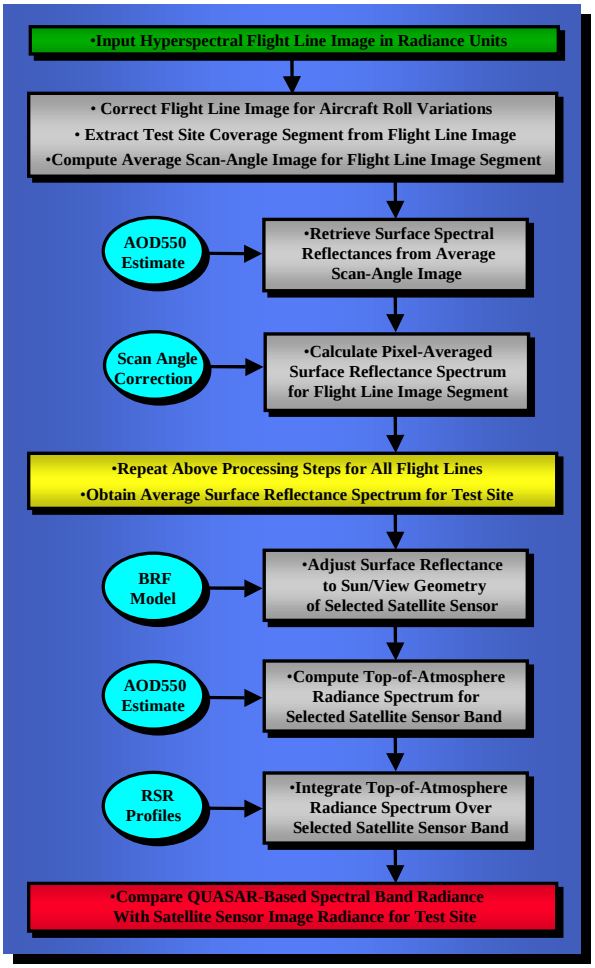

Figure 2. Detailed data flow scheme for the QUASAR monitoring method. AOD550 = aerosol optical depth at 0.550 micrometers, BRF = bi-directional reflectance factor, and RSR = relative spectral response.

Atmospheric correction parameters include the aforementioned AOD550 values obtained from ground-based measurements, standard model values for stratospheric ozone content, and atmospheric water vapour content derived from an optimization procedure in the ISDAS computations. Adjustments for illumination and viewing geometry differences were based on bi-directional reflectance factor (BRF) surface measurements at the RVPN test site and on the Chen-modified Roujean model for barren land for the NCRA test site (Chen and Cihlar, 1997).

V. METHODOLOGY VALIDATION RESULTS

For the data acquisition campaign at the RVPN test site, independent data acquisition by the airborne hyperspectral AVIRIS, the ground-based FieldSpec spectrometer, and the Reagan solar radiometer provided an opportunity to perform an initial validation of key elements of the QUASAR methodology.

Sunphotometer Measurements

As mentioned in Section III, AOD550 values retrieved from the Microtops-II and Reagan sunphotometer measurements at the RVPN test site typically agreed to within 0.01 and did not differ by more than 0.03 over the course of several days of observations. This represents reasonable agreement between sunphotometers.

Surface Spectral Reflectance

Figure 3 shows a comparison of surface reflectance spectra averaged over the 100-meter by 100-meter validation site and nearby areas at the RVPN test site. The four curves correspond to ground-based GER3700 and FieldSpec measurements and atmospherically-corrected *casi* and AVIRIS image data. The *casi*-based and AVIRIS-based surface reflectance spectra are from the half-way point in the processing data flow shown in Figure 2. The *casi* spectrum clearly differs from that obtained from the AVIRIS data as well as from both of the ground-based spectrometers. The discrepancy is likely due to calibration uncertainties in the *casi* data. The percent relative differences between the AVIRIS and the *casi* spectra are also plotted, indicating a discrepancy ranging from roughly 5 percent in the blue to approximately 10 percent in the red and near-infrared.

Band-Integrated Surface Reflectances

Figure 4 shows the same surface spectral reflectances integrated over 20 satellite sensor spectral bands, namely sensor (spectral bands): AVHRR (1-2), SPOT-4 VGT (1-3), OrbView-2 SeaWiFS (1-8), Landsat TM (1-4), and SPOT-1/2 HRV (1-3). GER3700, AVIRIS-based and *casi*-based surface reflectances in these satellite sensor spectral bands are plotted against the FieldSpec-based reflectances for the RVPN validation site. The ± 2 percent error bars represent the standard deviations of the measurement sets only and not measurement uncertainties. The agreement is generally within ± 2 percent except for the *casi*-based points and the bluest spectral band cases, which include SeaWiFS spectral bands 1-4 and TM spectral band 1. The worst case at the lower end of the graph in Figure 4 is SeaWiFS spectral band 1, which has a central wavelength of 0.412 micrometers. The wavelength ranges of the airborne and surface sensors do not adequately encompass the shorter wavelength

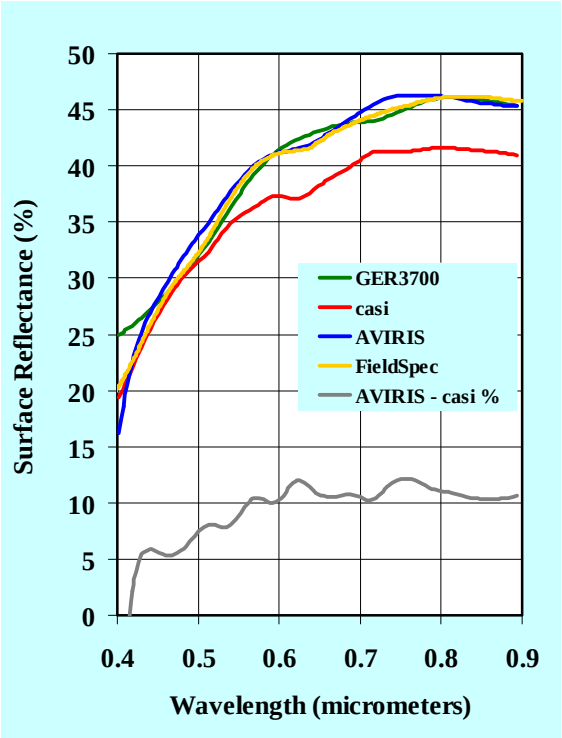

Figure 3. Percent surface spectral reflectance comparisons for the RVPN validation site. The lowest curve is the percentage relative difference between the AVIRIS and casi reflectance.

portions of the bluest satellite spectral bands under investigation. Nevertheless, the results shown in Figure 4 are reasonable given the completely independent data and methods involved. The slope of the GER3700 surface reflectances is 0.93 and the correlation between the GER3700 and FieldSpec reflectances has a coefficient of determination (r^2) of 0.99. The slopes of the AVIRIS-based and *casi*-based surface reflectances are 0.98 and 0.82, respectively, and the correlations between these reflectances and FieldSpec reflectances both have r^2 values of 0.99.

Calibration Correction for *casi*-Based Results

The methodology validation results clearly indicate a discrepancy in the *casi* calibration and, therefore, a correction is needed in order to use the *casi*-based results generated for the two NCRA campaigns. Since the AVIRIS is known to be a well-calibrated sensor and the same *casi* sensor was used in all three 1998 campaigns, the ratio spectrum shown in Figure 5 was used to correct the average *casi*-based surface reflectances obtained for the NCRA test site.

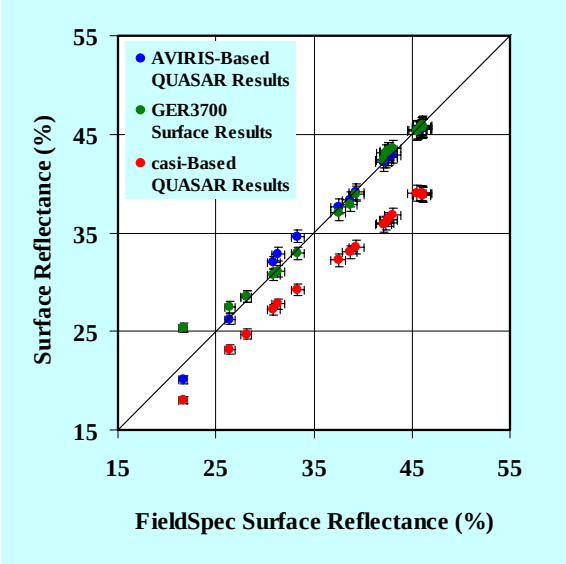

Figure 4. Percent surface reflectance comparisons in selected satellite sensor bands for the RVPN validation site. The ± 2 percent error bars represent standard deviations typical of the data sets. The diagonal line is the unity slope line.

VI. QUASAR MONITORING RESULTS

The key QUASAR results for each site consist of AVIRIS-based or *casi*-based TOA radiance estimates and their percentage differences with respect to satellite image-based TOA radiances determined independently using nominal post-launch calibration coefficients. The differences are defined as (QUASAR – nominal) / nominal in percent. This comparison is the final step in the processing data flow shown in Figure 2.

Results for the RVPN Test Site (June 17)

AVIRIS-based TOA radiance estimates were generated for NOAA-14 AVHRR spectral band 1, SPOT-4 VGT spectral bands 1 to 3, and OrbView-2 SeaWiFS spectral bands 1 to 8, which imaged the test site on the day of the airborne data acquisitions (June 17). The results are shown in Figure 6 and in Table 1, which includes the main observational parameters for the satellite sensor acquisitions. For 12 spectral bands from the three sensors, the QUASAR monitoring approach predicts TOA radiances that differ from the nominal TOA radiances by –3.3 to +7.3 percent (relative). The error bars in Figure 6 represent ± 6 percent uncertainty levels. For the QUASAR result axis, this corresponds to the error estimate of Scott et al. (1996) for cross-calibration

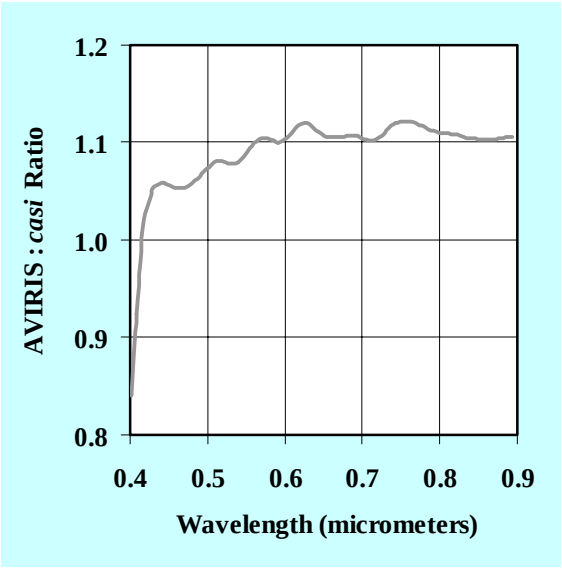

Figure 5. Ratio comparison of the surface reflectance spectra retrieved from the airborne AVIRIS and casi image data for the RVPN validation site.

Test Site	RVPN	RVPN	RVPN	RVPN	RVPN	RVPN
Date (1998)	Jun-17	Jun-17	Jun-17	Jun-17	Jun-17	Jun-17
Sensor	AVHRR	VGT	VGT	VGT	SeaWiFS	SeaWiFS
Spectral band	1	B0	B2	B3	1	2
Central wavelength (micrometers)	0.633	0.445	0.670	0.825	0.412	0.443
Solar zenith angle (degrees)	26.3	26.5	26.5	26.5	20.7	20.7
Satellite zenith angle (degrees)	43.9	43.0	43.0	43.0	58.7	58.7
Relative azimuth (degrees)	163.4	16.2	16.2	16.2	50.8	50.8
BRF adjustment factor	0.95	1.02	1.02	1.02	0.88	0.88
Δ TOA L* = % (Q - N)/N	7.3%	3.0%	5.5%	3.8%	-1.8%	-3.3%

Test Site	RVPN	RVPN	RVPN	RVPN	RVPN	RVPN
Date (1998)	Jun-17	Jun-17	Jun-17	Jun-17	Jun-17	Jun-17
Sensor	SeaWiFS	SeaWiFS	SeaWiFS	SeaWiFS	SeaWiFS	SeaWiFS
Spectral band	3	4	5	6	7	8
Central wavelength (micrometers)	0.490	0.510	0.555	0.670	0.765	0.865
Solar zenith angle (degrees)	20.7	20.7	20.7	20.7	20.7	20.7
Satellite zenith angle (degrees)	58.7	58.7	58.7	58.7	58.7	58.7
Relative azimuth (degrees)	50.8	50.8	50.8	50.8	50.8	50.8
BRF adjustment factor	0.88	0.88	0.88	0.88	0.88	0.88
Δ TOA L* = % (Q - N)/N	5.8%	4.8%	1.8%	-1.5%	-3.2%	2.3%

Table 1. QUASAR parameters and results for the airborne data acquisition day at the RVPN test site (June 17, 1998), where L is the top-of-atmosphere (TOA) radiance and Q and N refer to the QUASAR and nominal radiances, respectively.*

Test Site	NCRA	NCRA	NCRA	NCRA	NCRA	NCRA	NCRA	NCRA	NCRA
Date (1998)	Aug-4	Aug-4	Aug-4	Aug-4	Aug-4	Aug-4	Aug-4	Aug-4	Aug-4
Sensor	AVHRR	SeaWiFS	SeaWiFS	SeaWiFS	SeaWiFS	SeaWiFS	SeaWiFS	SeaWiFS	SeaWiFS
Spectral band	1	1	2	3	4	5	6	7	8
Central wavelength (micrometers)	0.633	0.412	0.443	0.490	0.510	0.555	0.670	0.765	0.865
Solar zenith angle (degrees)	37.5	34.7	34.7	34.7	34.7	34.7	34.7	34.7	34.7
Satellite zenith angle (degrees)	35.4	31.0	31.0	31.0	31.0	31.0	31.0	31.0	31.0
Relative azimuth (degrees)	136.8	40.0	40.0	40.0	40.0	40.0	40.0	40.0	40.0
BRF adjustment factor	0.88	1.20	1.20	1.20	1.20	1.20	1.20	1.20	1.20
Δ TOA L* = % (Q - N)/N	22.2%	-14.3%	-2.2%	-2.7%	10.0%	-8.4%	-3.2%	3.8%	4.6%

Test Site	NCRA	NCRA	NCRA	NCRA	NCRA	NCRA	NCRA	NCRA	NCRA
Date (1998)	Oct-4	Oct-4	Oct-4	Oct-4	Oct-4	Oct-4	Oct-4	Oct-4	Oct-4
Sensor	AVHRR	SeaWiFS	SeaWiFS	SeaWiFS	SeaWiFS	SeaWiFS	SeaWiFS	SeaWiFS	SeaWiFS
Spectral band	1	1	2	3	4	5	6	7	8
Central wavelength (micrometers)	0.633	0.412	0.443	0.490	0.510	0.555	0.670	0.765	0.865
Solar zenith angle (degrees)	61.7	55.2	55.2	55.2	55.2	55.2	55.2	55.2	55.2
Satellite zenith angle (degrees)	12.3	36.5	36.5	36.5	36.5	36.5	36.5	36.5	36.5
Relative azimuth (degrees)	141.0	57.4	57.4	57.4	57.4	57.4	57.4	57.4	57.4
BRF adjustment factor	0.88	1.29	1.29	1.29	1.29	1.29	1.29	1.29	1.29
Δ TOA L* = % (Q - N)/N	-3.7%	-15.1%	-3.6%	-6.9%	7.5%	-4.4%	-1.9%	5.6%	6.8%

Test Site	NCRA	NCRA	NCRA	NCRA	NCRA	NCRA	NCRA	NCRA	NCRA	NCRA
Date (1998)	Oct-4	Oct-4	Oct-4	Oct-4	Oct-4	Oct-4	Oct-4	Oct-4	Oct-4	Oct-4
Sensor	VGT	VGT	VGT	TM	TM	TM	TM	S2-HRV	S2-HRV	S2-HRV
Spectral band	B0	B2	B3	1	2	3	4	1	2	3
Central wavelength (micrometers)	0.445	0.670	0.825	0.486	0.571	0.661	0.838	0.549	0.653	0.840
Solar zenith angle (degrees)	56.5	56.5	56.5	57.3	57.3	57.3	57.3	55.4	55.4	55.4
Satellite zenith angle (degrees)	35.5	35.5	35.5	1.8	1.8	1.8	1.8	3.3	3.3	3.3
Relative azimuth (degrees)	60.0	60.0	60.0	53.4	53.4	53.4	53.4	115.6	115.6	115.6
BRF adjustment factor	1.45	1.45	1.45	1.00	1.00	1.00	1.00	1.00	1.00	1.00
Δ TOA L* = % (Q - N)/N	-13.2%	21.9%	24.3%	1.7%	15.8%	-0.5%	0.1%	-10.9%	-6.2%	-8.6%

Table 2. QUASAR parameters and results for the airborne data acquisition days for the NCRA test site (August 4 and October 4, 1998), where L is the top-of-atmosphere (TOA) radiance and Q and N refer to the QUASAR and nominal radiances, respectively.*

using the Railroad Valley playa. For the nominal calibration result axis, although the various satellite sensors involved have different calibration uncertainties, ± 6 percent has been used as a representative value. The slope of the 12 data points in Figure 6 is 1.08 and $r^2 = 0.95$.

Results for the NCRA Test Site (August 4)

Based on the data acquisition campaign at the NCRA test site on August 4, 1998, *casi*-based QUASAR monitoring results were obtained for NOAA-14 AVHRR spectral band 1 and OrbView-2 SeaWiFS spectral bands 1 to 8. Data processing and calibration corrections were as described in the previous Sections. As indicated in Figure 7 and Table 2, the QUASAR results for SeaWiFS are within 10 percent of nominal values except for spectral band 1, whereas the AVHRR result is well above nominal (+22 percent relative). Specific reasons for the AVHRR mismatch are not yet understood, but the most likely cause is thought to be an inadequate BRF adjustment. The slope of the 9 data points in Figure 7 is 0.67 and $r^2 = 0.83$.

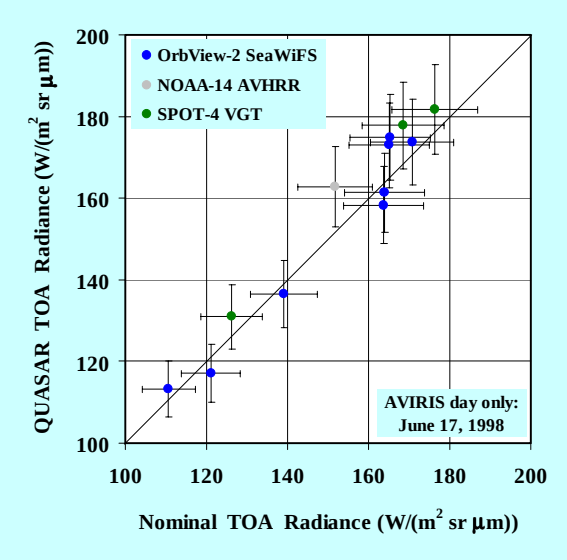

Figure 6. Comparison of QUASAR and nominal top-of-atmosphere (TOA) radiances for the RVPN test site for June 17, 1998. The satellite sensor cases include NOAA-14 AVHRR spectral band 1, SPOT-4 VGT spectral bands 1-3, and OrbView-2 SeaWiFS spectral bands 1-8. The error bars represent ±6 percent uncertainty levels. The diagonal line is the unity slope line. The slope of the data points is 1.08 and $r^2 = 0.95$.

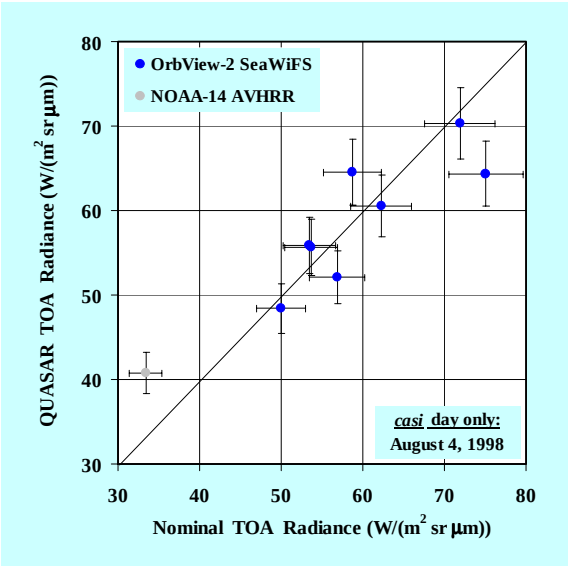

Figure 7. Comparison of QUASAR and nominal top-of-atmosphere (TOA) radiances for the NCRA test site for August 4, 1998. The satellite sensor cases include NOAA-14 AVHRR spectral band 1 and OrbView-2 SeaWiFS spectral bands 1-8. The error bars represent ± 6 percent uncertainty levels. The diagonal line is the unity slope line. The slope of the data points is 0.67 and $r^2 = 0.83$.

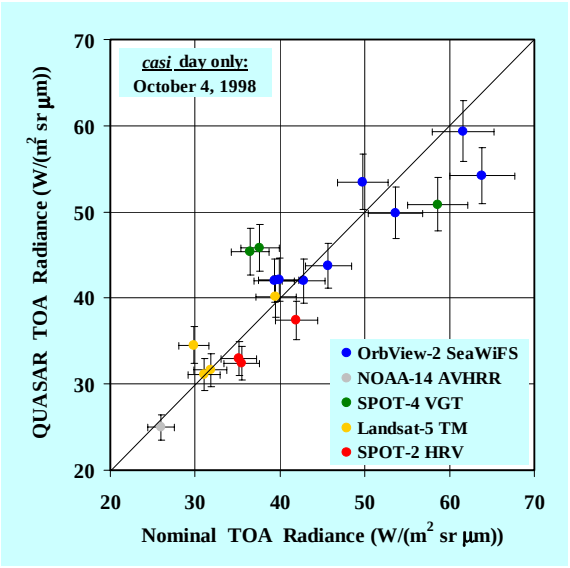

Figure 8. Comparison of QUASAR and nominal top-of-atmosphere (TOA) radiances for the NCRA test site for October 4, 1998. The satellite sensor cases include NOAA-14 AVHRR spectral band 1, SPOT-4 VGT spectral bands 1-3, OrbView-2 SeaWiFS spectral bands 1-8, Landsat-5 TM spectral bands 1-4, and SPOT-2 HRV spectral bands 1-3. The error bars represent ± 6 percent uncertainty levels. The diagonal line is the unity slope line. The slope of the data points is 0.76 and $r^2 = 0.81$.

Results for the NCRA Test Site (October 4)

Results for October 4 are shown in Figure 8 and Table 2. Five satellite sensors imaged the test site on that day. *casi*-based QUASAR monitoring results were generated for NOAA-14 AVHRR spectral band 1, OrbView-2 SeaWiFS spectral bands 1 to 8, SPOT-4 VGT spectral bands 1 to 3, Landsat-5 TM spectral bands 1 to 4, and SPOT-2 HRV spectral bands 1 to 3. As indicated in Figure 8 and Table 2, the QUASAR results for SeaWiFS are within 7.5 percent of nominal values except for spectral band 1, whereas the AVHRR result is close to the nominal value (-3.7 percent relative). Reasons for the larger mismatches for the VGT results are not yet understood. Results for TM are within a few percent of the nominal values, except for spectral band 2, and HRV results are within 11 percent of the nominal values. The slope of the 19 data points in Figure 8 is 0.76 and r^2 = 0.81. If the 28 data points in Figures 7 and 8 are combined, the slope of the TOA radiance comparison is 0.81 and r^2 = 0.87.

Discussion

Figures 9 and 10 summarise the QUASAR monitoring results obtained for the airborne data acquisition days at the two test sites. Five satellite sensors encompassing a total of 40 spectral band cases are included (Tables 1 and 2). The slope of the comparison between QUASAR-based and nominal TOA radiances is 1.03 and r^2 = 0.99. Thus, while problems arise in certain cases and the results for the NCRA test site show greater scatter, there is good correspondence overall between QUASAR-based and nominal radiometric calibration results. The use of the lower-radiance rangeland test site is beneficial in that the combined data set yields a better radiance correlation than do the individual test sites processed separately. Figure 10 plots the percent relative difference between the QUASAR-based and nominal calibrations as a function of the nominal TOA radiance values. Greater differences for the lower-radiance NCRA test site than for the RVPN test site are consistent with a roughly constant error in absolute radiance terms.

The main error source contributing to the scatter in the QUASAR results is considered to be attributable to inadequate BRF adjustments. Confirmation that this is the main error source will require further study. There are also uncertainties in the nominal calibrations, but their discussion is beyond the scope of this paper.

The 40 spectral band cases that make up the current QUASAR monitoring results have been examined as a function of the five observational parameters listed in Tables 1 and 2. I.e., Δ TOA L* was plotted (not shown), in turn, as a function of central wavelength, solar zenith angle, satellite zenith angle, relative azimuth, and BRF adjustment factor. No significant trends were found. On the basis of the 40 cases examined, it is tentatively concluded that the QUASAR approach is not sensitive in any systematic way to any of these observational parameters.

VII. TEMPORAL EXTENSIONS TO OTHER DAYS

The availability of satellite imagery within a few days of the airborne data acquisition days made it possible to consider temporal extensions of the QUASAR monitoring results. In these cases, the atmospheric parameters used in the processing pertain to those that were estimated on the airborne data acquisition day and they are assumed to remain unchanged for the other days. The test site surface is also assumed to have remained unchanged. Clearly, these assumptions are potential sources of error in extending results temporally and, in due course, the trade-off between more data points and reduced accuracy will have to be examined. On the other hand, in the QUASAR processing, actual illumination and viewing geometries pertinent to each satellite sensor image acquisition were used and an appropriate BRF adjustment factor was computed and used accordingly.

Results for the RVPN Test Site (June)

QUASAR TOA radiances estimates for AVHRR cases on other dates around the airborne data acquisition day (June 18-22) differ increasingly from the June 17 result as a function of temporal extension. TOA radiance differences as previously defined change systematically from +7.3 percent on June 17 to –13.0 percent on June 22 (Figure 11). Such a trend is consistent with an increase in surface reflectance with a drying playa over time and/or increasingly hazier atmospheric conditions over time. Increased surface reflectance and/or increased atmospheric contribution in visible spectral bands would lead to higher nominal TOA radiances compared to the QUASAR values obtained on the airborne data acquisition day. Contrary to this trend, for unknown reasons, results for the eight SeaWiFS spectral bands for June 18 differ from nominal values by an average of +16 percent.

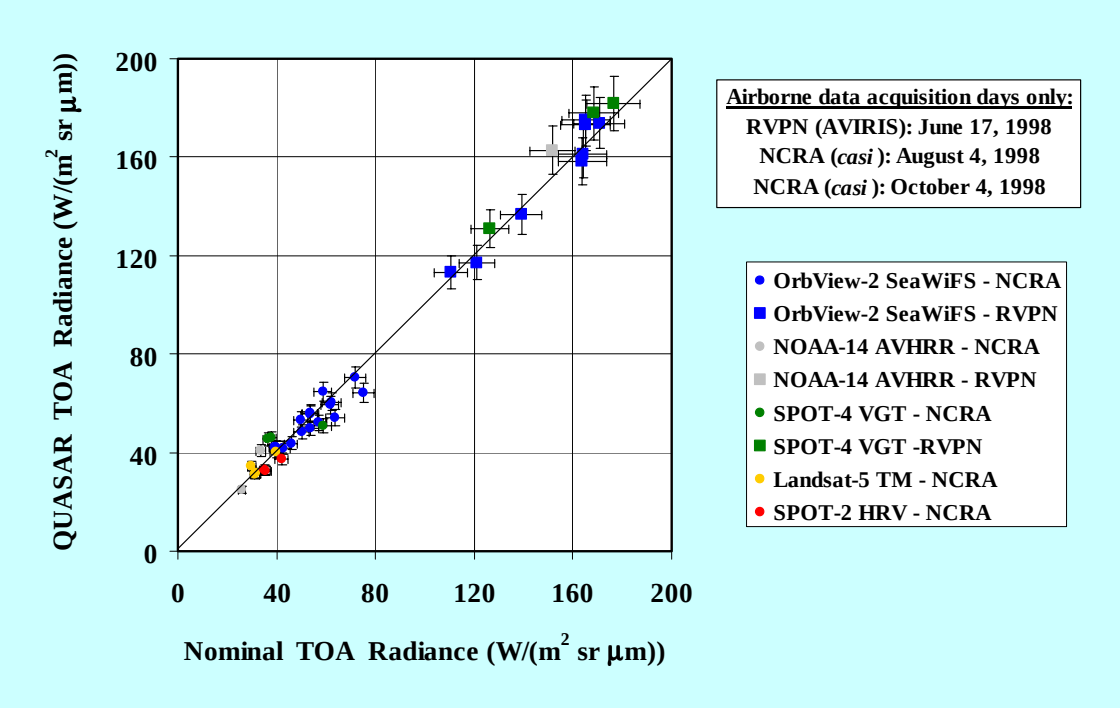

Figure 9. Comparison of QUASAR and nominal top-of-atmosphere (TOA) radiances for the three airborne data acquisition days (one at the RVPN test site and two at the NCRA test site). The satellite sensor cases include NOAA-14 AVHRR spectral band 1, SPOT-4 VGT spectral bands 1-3, OrbView-2 SeaWiFS spectral bands 1-8, Landsat-5 TM spectral bands 1-4, and SPOT-2 HRV spectral bands 1-3. The error bars represent ± 6 percent uncertainty levels. The diagonal line is the unity slope line. The slope of the data points is 1.03 and $r^2 = 0.99$.

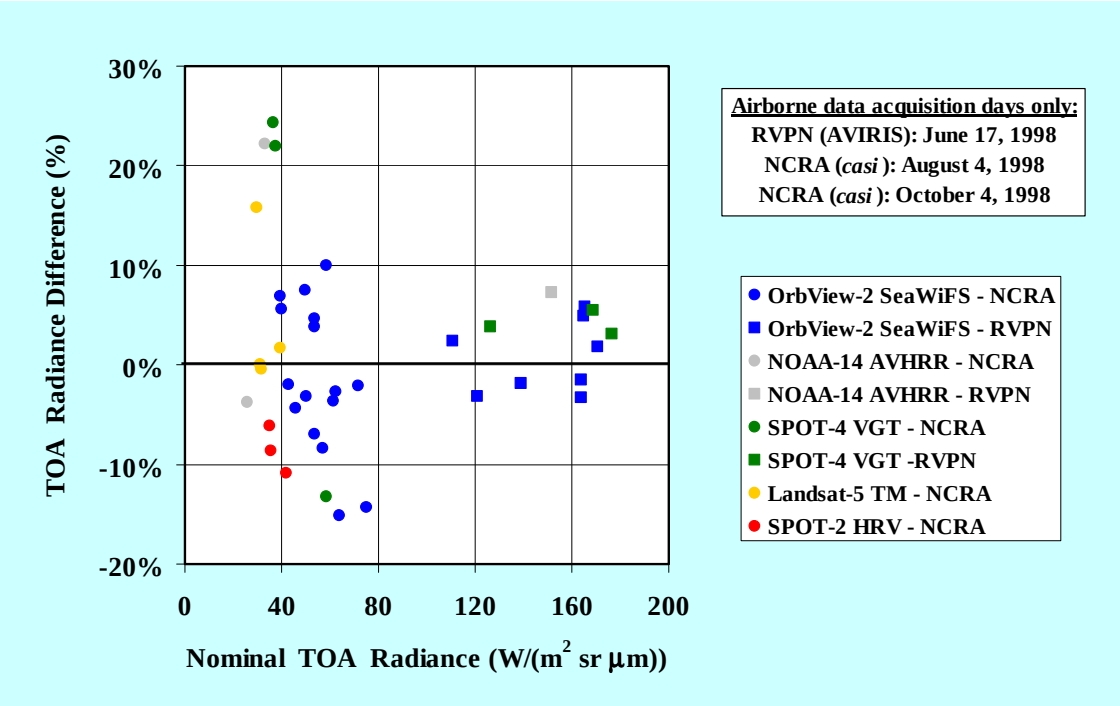

Figure 10. Percent relative difference between the QUASAR and nominal top-of-atmosphere (TOA) radiances as a function of the nominal values based on the three data acquisition campaigns (one at the RVPN test site and two at the NCRA test site). The satellite sensor cases are the same as for Figure 9.

With respect to small footprint sensors TM and HRV, neither of the satellite sensor data sets was acquired on the same day as the airborne hyperspectral data acquisition. Therefore, the generation of QUASAR monitoring results in these cases relies exclusively on temporal extrapolations of surface and atmospheric conditions ranging from one to three days. Results for the four TM spectral bands for June 14 differ from nominal values by an average of +23 percent. Results for the three SPOT-1 HRV spectral bands for June 18 differ from nominal values by an average of -15 percent. Thus, the RVPN QUASAR data sets do not provide a good reference for Landsat-5 TM three days earlier (June 14) and SPOT-1 HRV a day later (June 18). This situation is likely to be due at least in part to significant changes in the playa surface while it was drying after a rainy period earlier in the month. The days following a wet period should be avoided and/or a better knowledge of the characteristics of the RVPN test site as a function of time needs to be developed.

Results for the NCRA Test Site (August)

QUASAR TOA radiances estimates for SeaWiFS cases on other dates around the airborne data acquisition day (August 6-10) also differ increasingly from the August 4 results as a function of temporal extension. Figure 11 shows this trend for the red spectral band (SeaWiFS band 6) in order to facilitate inter-comparison with temporal trends in results for AVHRR. Similarly, results for several AVHRR cases on other dates around the airborne data acquisition day (August 6-10) differ from nominal values by varying amounts (Figure 11).

Neither of the data sets from the small footprint satellite sensors was acquired on the same day as the airborne hyperspectral data acquisitions. For TM data acquired four days after the *casi* data acquisition (August 8), matches in the range of –2.7 to +8.7 percent were obtained. The QUASAR results for SPOT-2 HRV on August 7 predict TOA radiances –5.4 to –2.4 percent lower than nominal radiances.

Results for the NCRA Test Site (October)

The QUASAR TOA radiance estimate for AVHRR on October 5 differs from the nominal value by –7.2 percent, similar to the result obtained on the airborne data acquisition day (October 4). The VGT results on October 3 are closer to nominal values than the VGT results on October 4, ranging from –6.8 to +10.9 percent. SeaWiFS cases on other dates around the airborne data acquisition day (October 5-8) differ increasingly from nominal values as a function of temporal extension (Figure 11).

Discussion

It is clear from the above results that temporal extensions of a few days do not necessarily provide calibration redundancy and may even create higher levels of uncertainty. The temporal trends obtained can be caused by changes in surface conditions, atmospheric conditions, and/or observation geometries affecting BRF adjustments, but little more can be said in the absence of ground-based measurements on these days.

An overview of the main QUASAR results (40 cases) and the temporal extension results (86 cases) is presented in Table 3. Absolute values of the relative differences between QUASAR and nominal TOA radiances were averaged to generate the excursions given in the table. On the left-hand side of the table, the averages are over the number of spectral band cases. On the right-hand side, the averages are weighted by the number of satellite sensor cases, which gives each satellite sensor equal weight

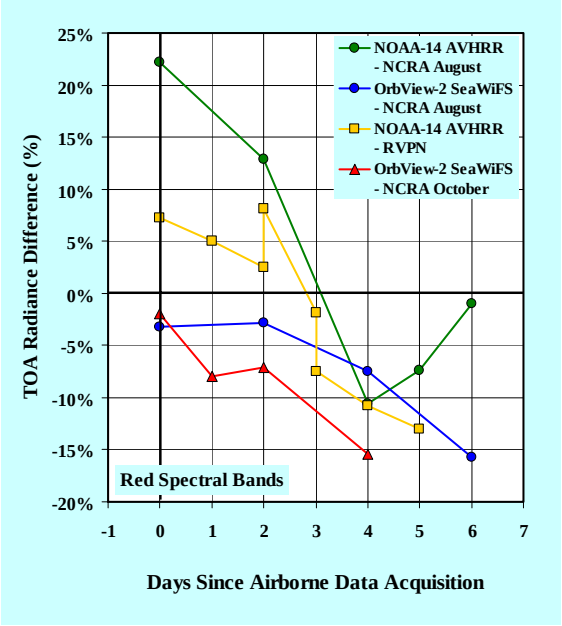

Figure 11. Percent relative difference between the QUASAR and nominal top-of-atmosphere (TOA) radiances as a function of temporal extension in days since airborne data acquisition. Only red spectral bands (i.e., near 0.65 micrometers) are included. Points are connected as a visual aid only. Day zero is the day of the airborne data acquisition for each of the three test site campaigns.

Airborne Data Acquistion Days							Airborne Data Acquistion Days						
Satellite Sensor	RVPN		NCRA		Both Sites		Satellite Sensor	RVPN		NCRA		Both Sites	
	Average TOA Radiance Excursion	Number of Spectral Band Cases	Average TOA Radiance Excursion	Number of Spectral Band Cases	Average TOA Radiance Excursion	Number of Spectral Band Cases		Average TOA Radiance Excursion	Number of Satellite Sensor Cases	Average TOA Radiance Excursion	Number of Satellite Sensor Cases	Average TOA Radiance Excursion	Number of Satellite Sensor Cases
AVHRR	7.3%	1	13.0%	2	11.1%	3	AVHRR	7.3%	1	13.0%	2	11.1%	3
VGT	4.1%	3	19.8%	3	12.0%	6	VGT	4.1%	1	19.8%	1	12.0%	2
TM			4.5%	4	4.5%	4	TM			4.5%	1	4.5%	1
HRV			8.5%	3	8.5%	3	HRV			8.5%	1	8.5%	1
SeaWiFS	3.1%	8	6.3%	16	5.2%	24	SeaWiFS	3.1%	1	6.3%	2	5.2%	3
Overall:	**3.7%**	**12**	**8.2%**	**28**	**6.9%**	**40**	**Overall:**	**4.8%**	**3**	**10.2%**	**7**	**8.6%**	**10**
Other Days							**Other Days**						
Satellite Sensor	RVPN		NCRA		Both Sites		Satellite Sensor	RVPN		NCRA		Both Sites	
	Average TOA Radiance Excursion	Number of Spectral Band Cases	Average TOA Radiance Excursion	Number of Spectral Band Cases	Average TOA Radiance Excursion	Number of Spectral Band Cases		Average TOA Radiance Excursion	Number of Satellite Sensor Cases	Average TOA Radiance Excursion	Number of Satellite Sensor Cases	Average TOA Radiance Excursion	Number of Satellite Sensor Cases
AVHRR	6.9%	8	7.8%	5	7.3%	13	AVHRR	6.9%	8	7.8%	5	7.3%	13
VGT			9.5%	3	9.5%	3	VGT			9.5%	1	9.5%	1
TM	24.8%	4	5.1%	4	14.9%	8	TM	24.8%	1	5.1%	1	14.9%	2
HRV	14.9%	3	3.8%	3	9.3%	6	HRV	14.9%	1	3.8%	1	9.3%	2
SeaWiFS	16.0%	8	11.8%	48	12.4%	56	SeaWiFS	16.0%	1	11.8%	6	12.4%	7
Overall:	**14.2%**	**23**	**10.6%**	**63**	**11.6%**	**86**	**Overall:**	**15.6%**	**11**	**9.2%**	**14**	**12.0%**	**25**
All Days							**All Days**						
Satellite Sensor	RVPN		NCRA		Both Sites		Satellite Sensor	RVPN		NCRA		Both Sites	
	Average TOA Radiance Excursion	Number of Spectral Band Cases	Average TOA Radiance Excursion	Number of Spectral Band Cases	Average TOA Radiance Excursion	Number of Spectral Band Cases		Average TOA Radiance Excursion	Number of Satellite Sensor Cases	Average TOA Radiance Excursion	Number of Satellite Sensor Cases	Average TOA Radiance Excursion	Number of Satellite Sensor Cases
AVHRR	7.0%	9	9.3%	7	8.0%	16	AVHRR	7.0%	9	9.3%	7	8.0%	16
VGT	4.1%	3	14.7%	6	11.1%	9	VGT	4.1%	1	14.7%	2	11.1%	3
TM	24.8%	4	4.8%	8	11.5%	12	TM	24.8%	1	4.8%	2	11.5%	3
HRV	14.9%	3	6.2%	6	9.1%	9	HRV	14.9%	1	6.2%	2	9.1%	3
SeaWiFS	9.5%	16	10.4%	64	10.3%	80	SeaWiFS	9.5%	2	10.4%	8	10.3%	10
Overall:	**10.6%**	**35**	**9.9%**	**91**	**10.1%**	**126**	**Overall:**	**12.0%**	**14**	**9.5%**	**21**	**10.5%**	**35**

Table 3. Average excursions of QUASAR TOA radiances from nominal values: averaged over the number of spectral band cases (left-hand side); weighted over the number of satellite sensor cases (right-hand side). An excursion is defined as the absolute value of the relative difference between QUASAR and nominal TOA radiances.

regardless of the number of spectral band cases included in the results for that sensor. The table indicates that the RVPN test site yields lower relative excursions overall than does the NCRA test site, which is consistent with the higher radiances characteristic of the former. The table also indicates that the RVPN results change more with temporal extensions.

Based on Table 3, the average excursions for the main QUASAR results at the RVPN and NCRA test sites are in the 4 to 5 percent range and in the 8 to 10 percent range, respectively. Since these excursions are with respect to nominal calibration results, which have their own uncertainty, they are not a measure of the absolute error associated with the QUASAR approach. Nevertheless, the results are in keeping with the $\pm$ 6 percent estimate of Scott et al. (1996) for cross-calibration using the Railroad Valley playa.

VIII. CONCLUDING REMARKS

An experimental QUASAR monitoring methodology has been developed and tested at the RVPN and NCRA test sites. QUASAR monitoring results have been generated for six satellite sensors based on airborne hyperspectral data acquisition campaigns at the Railroad Valley playa test site in Nevada in June 1998 and the Newell County rangeland test site in Alberta in August and October 1998. The main results consist of AVIRIS-based and *casi*-based TOA radiance predictions and their percentage difference comparisons with satellite-based TOA radiances determined independently using nominal post-launch calibration coefficients.

Measurements and processing results based on the chosen sensor set for experimental QUASAR monitoring (Microtops-II, GER3700, and *casi*) were validated against independent sensor results at the RVPN test site (Reagan, FieldSpec, and AVIRIS). Consistent results were obtained in all cases except for *casi*-based QUASAR reflectances, which indicated a *casi* radiometric calibration problem. A calibration correction was generated using the AVIRIS:*casi* reflectance ratio for the RVPN test site in order to correct the *casi*-based QUASAR results obtained at the NCRA test site.

For QUASAR monitoring based on the same-day reference data set for the RVPN test site, there is good agreement between QUASAR-based and nominal TOA radiances, with average excursions from nominal in the range of 4 to 5 percent (relative). For 12 spectral band cases, the TOA radiance

comparison is characterised by a slope of 1.08 and a coefficient of determination (r^2) of 0.95. Compared to the RVPN results, there is less agreement between QUASAR-based and nominal TOA radiances for the NCRA test site, with average excursions from nominal in the range of 8 to 10 percent (relative). For 28 spectral band cases, the TOA radiance comparison is characterised by a slope of 0.81 and r^2 = 0.87. For the combined results from the RVPN and NCRA test sites (40 spectral band cases), the general agreement between QUASAR-based and nominal TOA radiances is characterised by a slope of 1.03 and r^2 = 0.99. Thus, while the NCRA results have apparently inferior statistics, the use of the lower-radiance rangeland test site improves the TOA radiance comparison that constitutes the main QUASAR monitoring result. The collective results also indicate that the nominal on-orbit radiometric calibrations of all the satellite sensors fit within their predicted uncertainties.

Based on the 40 spectral band cases examined, the QUASAR approach is not sensitive in any systematic way to wavelength, illumination and observation angles, and BRF adjustment factor. The main source of error is very likely inadequate knowledge of the surface BRF. The use of a rangeland test site for QUASAR monitoring will require better characterisation of surface reflectance anisotropies.

Temporal extensions of QUASAR data sets to days near to the airborne data acquisition day yield mixed results. The RVPN results are more affected by temporal extensions than are the NCRA results. In general, one must be wary of the trade-off between calibration data redundancy offered by temporal extensions and validation degradation induced by significant day-to-day changes in test site conditions.

Overall, the results obtained to date are sufficiently promising that, with careful refinements, the QUASAR methodology has the potential to become a generalized approach to vicarious calibration. The approach constitutes a worthwhile validation exercise that generates useful and informative radiometric calibration redundancy when applied to a number of Earth observation satellite sensors.

Future activities currently envisaged include QUASAR monitoring tests for post-launch Landsat-7 Enhanced Thematic Mapper Plus (ETM+) and EO-1 and EOS Terra sensor cases, additional radiometric uniformity studies of the RVPN and NCRA test sites, and a full radiometric error analysis of the QUASAR method. There is a definite need for further work on the bi-directional reflectance characteristics of optical sensor calibration test sites. An intercomparison of the QUASAR monitoring method with respect to independent vicarious calibration techniques also remains to be done.

IX. ACKNOWLEDGEMENTS

The authors gratefully acknowledge the technical assistance of Prabal Nandy and John Lamarr (University of Arizona) regarding BRDF and FieldSpec measurements, respectively, at the Railroad Valley playa, Julie Lefebvre (MacDonald Dettwiler and Associates) with respect to ISDAS processing issues, Karen S. Baith (NASA Goddard Space Flight Center) with respect to SeaDAS processing, and Marie-Christine Laubies and Frédérique Meunier (Centre national d'études spatiales (CNES)) with respect to VGT specifications.

X. REFERENCES

Bergeron, M., O'Neill, N.T., Royer, A., and Teillet, P.M., "Development of a Spectral Error Model for Surface Bidirectional Reflectance Factor (BRF) Retrieval", *Canadian Journal of Remote Sensing*, **24(2):** 128-132, 1998.

Biggar, S.F., Slater, P.N., and Gellman, D.I., "Uncertainties in the In-Flight Calibration of Sensors With Reference to Measured Ground Sites in the 0.4 to 1.1 mm Range", *Remote Sensing of Environment*, **48:** 242-252, 1994.

Chen, J.M., and Cihlar, J., "A Hotspot Function in a Simple Bidirectional Reflectance Model for Satellite Applications", *Journal of Geophysical Research*, **102(D22):** 25907-25913, 1997.

Fu, G., Baith, K.S., and McClain, C.R., "SeaDAS: The SeaWiFS Data Analysis System", *Proceedings of the 4th Pacific Ocean Remote Sensing Conference*, Qingdao, China, pp. 73-77, 1998.

Scott, K.P., Thome, K.J., and Brownlee, M.R., "Evaluation of the Railroad Valley Playa for Use in Vicarious Calibration", *Proceedings of SPIE Conference 2818*, Denver, Colorado, 1996.

Staenz, K., and Williams, D.J., "Retrieval of Surface Reflectance from Hyperspectral Data Using a Look-up Table Approach", *Canadian Journal of Remote Sensing*, **23(4):** 354-368, 1997.

Staenz, K., Szeredi, T., and Schwarz, J., “ISDAS – A System for Processing / Analyzing Hyperspectral Data”, *Canadian Journal of Remote Sensing*, **24(2):** 99-113, 1998.

Teillet, P.M., Fedosejevs, G., and Gauthier, R.P., "Operational Radiometric Calibration of Broadscale Satellite Sensors Using Hyperspectral Airborne Remote Sensing of Prairie Rangeland: First Trials", *Metrologia*, **35:**639-641, 1998a.

Teillet, P.M., Fedosejevs, G., Gauthier, R.P., and Schowengerdt, R.A., “Uniformity Characterization of Land Test Sites Used for Radiometric Calibration of Earth Observation Sensors”, *Proceedings of the Twentieth Canadian Symposium on Remote Sensing*, Calgary, Alberta, pp. 1-4, 1998b.

Teillet, P.M., Fedosejevs, G., Gauthier, R.P., O’Neill, N.T., Thome, K.J., Biggar, S.F., Ripley, H., and Meygret, A., "Radiometric Calibration of OrbView-2 SeaWiFS and SPOT-4 Vegetation Using Airborne Hyperspectral Data", *Proceedings of the Fourth International Airborne Remote Sensing Conference and Exhibition and the Twenty-First Canadian Symposium on Remote Sensing*, Ottawa, Ontario, in press, 8 pages, 1999a.

Teillet, P.M., Fedosejevs, G., Gauthier, R.P., Shin, R.T., N.T. O’Neill, N.T., Thome, K.J., Biggar, S.F., Ripley, H., and Meygret, A., "Radiometric Calibration of Multiple Earth Observation Sensors Using Airborne Hyperspectral Data at the Newell County Rangeland Test Site", *Proceedings of the SPIE Conference on Earth Observing Systems IV, SPIE Volume 3750*, Denver, Colorado, pp. 470-481, 1999b.

Teillet, P.M., Fedosejevs, G., Gauthier, R.P., O’Neill, N.T., Thome, K.J., Biggar, S.F., Ripley, H., and Meygret, A., "A Generalized Approach to the Vicarious Calibration of Multiple Earth Observation Sensors Using Hyperspectral Data", *Remote Sensing of Environment*, in press, 2000.

Vermote E.F., and Kaufman, Y.J., “Absolute Calibration of AVHRR Visible and Near-Infrared Channels Using Ocean and Cloud Views”, *International Journal of Remote Sensing*, **16(13):** 2317-2340, 1998.